

STATISTICAL AND OVERALL UNCERTAINTIES IN PROTON THERAPY MICRODOSIMETRIC MEASUREMENTS

D. Moro, E. Seravalli and P. Colautti

LNL-INFN, viale dell'Università 2. I-35020 Legnaro. Italy.

1. Introduction

In experimental microdosimetry, tissue equivalent gas proportional counters (TEPC) are used to measure pulse height spectra (microdosimetric spectra), that means ionisation event spectra generated by the radiation in a given site, which has generally 1 μm of size. The way to generate microdosimetric spectra is well described in ICRU Report 36 [1].

The usual representation of a microdosimetric spectrum is a semi-logarithmic plot, where the abscissa is the logarithm of the lineal energy $\ln(y)$ [$\text{keV}/\mu\text{m}$] and the ordinate is the product $yd(y)$ (where y is the lineal energy and $d(y)$ is the weighted distribution of y). The microdosimetric spectrum is usually processed to obtain the mean values $\overline{y_f}$ (the mean lineal energy), $\overline{y_d}$ (the weighted-mean lineal energy) and RBE_μ (the relative biological efficiency). In this paper we will analyse the overall uncertainty of the means, taking into account the count statistics as well as the lineal energy calibration uncertainty and the spectrum extrapolation uncertainty.

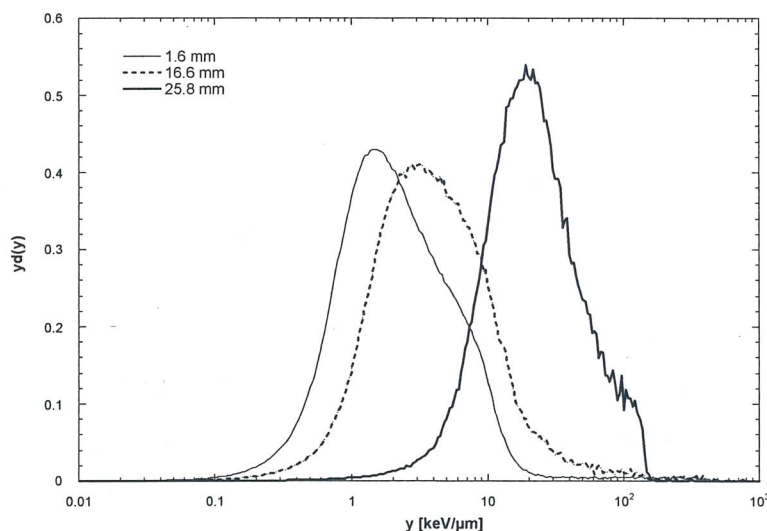


Figure 1. Microdosimetric spectra in a therapeutic proton beam. Thin line: entrance. Thick line: SOBP proximal edge. Thicker line: SOBP distal edge.

In fact, because of the electronic noise, the TEPC efficiency in measuring y -events is less than 1, depending on the low detection threshold, which usually ranges between 0.1 and 0.5 $\text{keV}/\mu\text{m}$. Spectra are therefore linearly extrapolated down to 0.01 $\text{keV}/\mu\text{m}$ before processing the data.

In this paper, we will analyse the mean overall uncertainties of the measurements performed at CATANA proton beam facility, which uses 60 MeV proton beams to treat eye melanomas. An example of proton spectra, collected at the CATANA therapeutic facility (located at Catania in Sicily), is in figure 1, where three microdosimetric spectra, collected at different depths in the therapeutic spread-out Bragg peak (SOBP), are shown. The three spectra have been collected at the beam entrance, at the SOBP proximal edge and at the SOBP distal edge. Increasing the depth, the absorbed dose is more and more due to bigger y -events, because of the proton mean energy decrease. Protons cannot give rise to events larger than about $150 \text{ keV}/\mu\text{m}$, which corresponds to the maximum of proton stopping power in propane-based tissue-equivalent gas mixture used in the TEPC. Events of larger size are due to heavier ions emerging from nuclear reactions.

A microdosimetric spectrum is originally collected on three different multi channel analysers. In fact, preamplifier pulses are sent to three different linear amplifiers, which have different gains in order to have the same resolution both for small-size y -events and large-size y -events. The three original sub-spectra, calibrated in Volt, are then joined and processed to have the same number of channels per y decade (the usual number of channels is 60, but any number can be chosen). Therefore, any channel in a microdosimetric spectrum has the same *logarithmic size*. The full spectrum has $n(\tilde{y}) \cdot \Delta\tilde{y}$ counts per channel, where the symbol \tilde{y} means that the lineal energy is in V and $\Delta\tilde{y}$ is the channel size. The spectrum is eventually recalibrated in lineal energy.

2. Statistical errors

The statistics of a therapeutic-proton beam microdosimetric spectrum varies with the lineal energy size. The statistic range is very large, since events with $y > 150 \text{ keV}/\mu$ (counts beyond the proton edge) have a rate of occurrence about 10^8 times less than that one of $0.1 \text{ keV}/\mu\text{m}$ events. The standard deviation (SD) has been taken as count uncertainty, which is, applying the Poisson statistics, the count square root. In figure 2 and 3, two of CATANA microdosimetric spectra (not extrapolated) of figure 1, are plotted together with the statistical uncertainty ($\pm 1 \text{ SD}$) of any channel content. As expected, the count relative standard-deviation varies a lot, being less than 1% for small y -values and 100% for large y -values where only one count has been collected.

3. Systematic errors

The average values $\overline{y_f}$, $\overline{y_d}$ and RBE_μ are calculated by applying an algorithm to the microdosimetric spectrum. Therefore, they are affected both by the count statistical uncertainty and by the uncertainty of the factors and the quantities used in the algorithm. We call the last ones

systematic errors. These errors can be minimised, but not eliminable. We have analysed three systematic error sources and their impact on the average-value overall uncertainty:

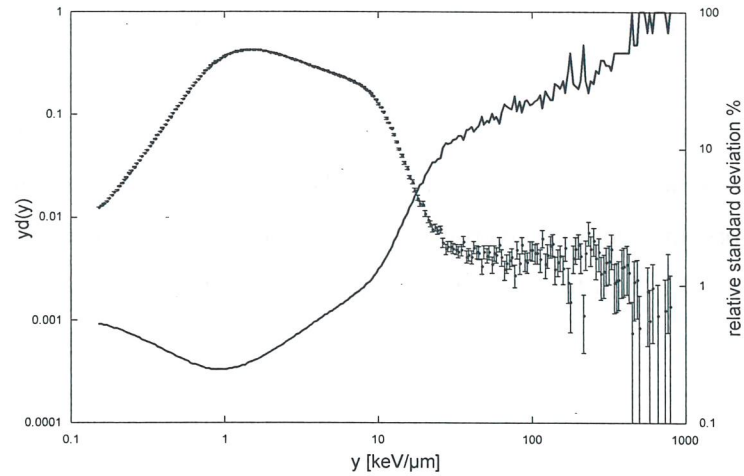


Figure 2. Microdosimetric spectrum (measured values only) at the SOBP entrance (1.6 mm of depth) with statistical uncertainties (± 1 SD). The count relative standard deviation (continuous line) is plotted on the right ordinate. The spectrum statistics is of $9.1 \cdot 10^6$ counts.

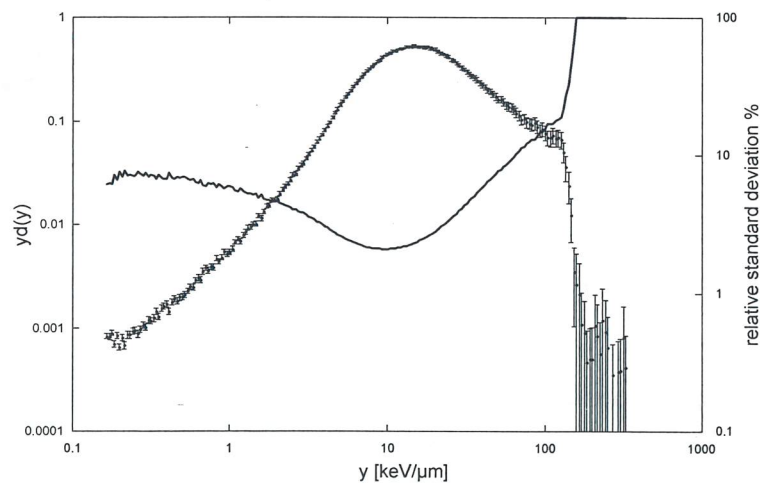


Figure 3. Microdosimetric spectrum (measured values only) at the SOBP distal edge (25.8 mm of depth) with statistical uncertainties (± 1 SD). The count relative standard deviation (continuous line) is plotted on the right ordinate. The spectrum statistics is of $1.6 \cdot 10^5$ counts.

1. the lineal energy calibration of the spectrum;
2. the spectrum extrapolation down to $0.01 \text{ keV}/\mu\text{m}$;
3. the weighting function $r(y)$, used to calculate the relative biological efficiency (RBE_μ)

3.1. Lineal energy calibration uncertainty

Because of the TEPC mini size, the use of an internal alpha calibration source for lineal energy calibration is uncomfortable. However, microdosimetric spectra can be self-calibrated by using the proton edge, the value of which can be calculated. From the table of stopping power [2], we have calculated that in $1\mu\text{m}$ of simulated diameter the maximum energy lost in propane-base tissue-equivalent gas mixture is 98 keV and consequently the lineal energy corresponding to the proton edge is $147\text{ keV}/\mu\text{m}$. Accordingly to ICRU49, the proton edge value error is mainly due to systematic errors. In order to convert estimated systematic errors in standard deviations, the factor 0.5 is used [2, 3, 4]. Therefore, the proton edge value is affected by the 3% of uncertainty.

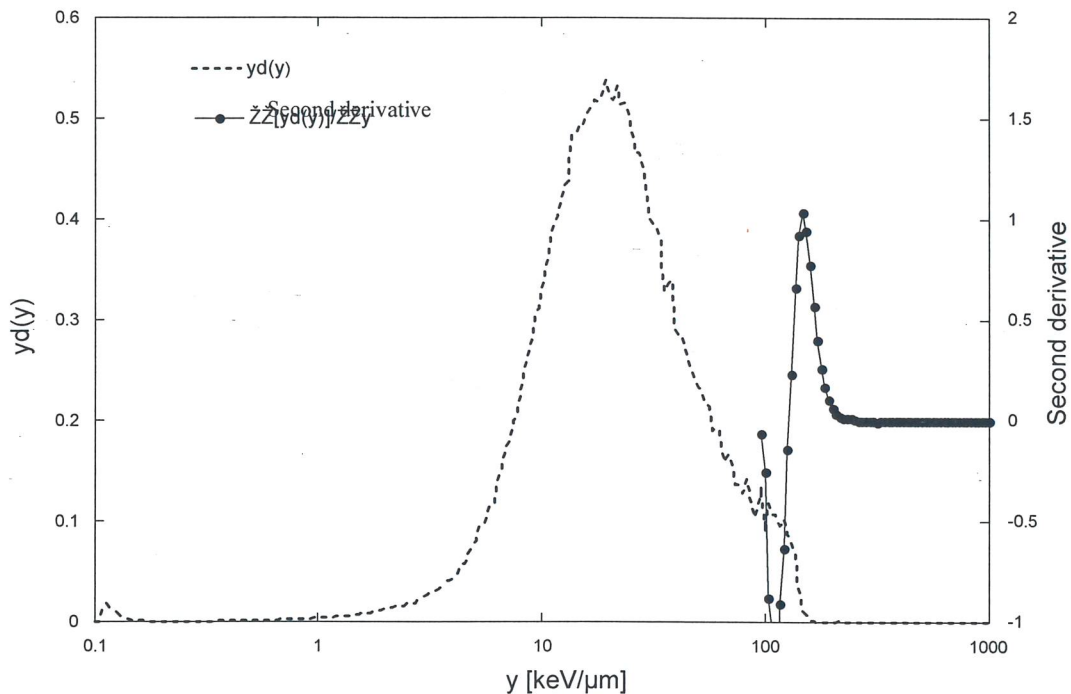


Figure 4. Microdosimetric spectrum at the SOBP distal edge (dashed line) and the second derivative of the same spectrum (line). The derivative values for $y < 95\text{ keV}/\mu\text{m}$ have been masked.

The lineal energy calibration procedure has another source of error; it is the uncertainty regarding the channel, given in V, at which the proton edge value has to be associated. The proton edge is in fact masked by the energy absorption fluctuation as well as by a population of events due to straggling protons and nuclear reaction products. We have followed the procedure to smooth the no-normalised weighted distribution $\tilde{y}^2 n(\tilde{y})$ and to derivate it twice. The smoothing is necessary to minimise the stochastic fluctuations, which mask the physics that means the end of those events which mainly populate that region, giving rise at the proton edge. However,

increasing the smoothing decreases the y resolution. A compromise has to be found. Eventually, the second derivative shows a clear maximum at the proton edge position (see figure 4). The uncertainty of the second derivative maximum position has been taken as the half of the interval $\Delta\tilde{y}$. That means ~ 3 keV/ μm for a 60 channels per decade spectrum. Therefore, the individuation of the peak maximum has a relative uncertainty of the 2%.

The calibration overall uncertainty can be estimated by summing the squared standard deviations and making the squared root of the sum. Therefore, the overall relative uncertainty results to be 3.6%. Comparison with the traditional alpha source calibration method [5] shows that differences are smaller than the estimated overall uncertainty.

3.2. Spectrum extrapolation uncertainty

Microdosimetric spectra have a low detection threshold, which depends on the electronic noise and on the counter gas gain. Measurements performed with mini TEPCs at CATANA had a threshold between 0.1 and 0.2 keV/ μm (see figure 4). Therefore, in order to properly calculate the microdosimetric average values, it is necessary to assess the lacking part of the spectrum. We have chosen to extrapolate linearly the last part of the pulse-height frequency spectrum down to \tilde{y}_{\min} -value, which corresponds to 0.01 keV/ μm .

One-way to access the uncertainty on the extrapolation is performing two different extrapolations: the first one drawing a line of slope 0 from the last noise-free point and the second one by best-fitting the last 5 noise-free points. However, this way depends on the frequency spectrum slope at the threshold. Therefore, we have chosen the more drastic assessment of considering all the extrapolated part as a systematic uncertainty. The extrapolation systematic uncertainty (in following processed as a standard deviation dividing by 2 the systematic uncertainty [3, 4]) is assumed to be the mean value calculated from \tilde{y}_{\min} and \tilde{y}_{thr} , where \tilde{y}_{thr} is the low threshold value.

3.3. Weighting function uncertainty

RBE is a radiobiological measurement, microdosimetric experimental data can be used to assess *RBE* by using a suitable weighting function $r(y)$. We call the microdosimetric-calculated *RBE* value RBE_{μ} . It is defined as:

$$RBE_{\mu} = \sum_{0.01}^{y_{\max}} r(y_i) \cdot d(y_i) \cdot \Delta y_i \quad (1)$$

$r(y)$ is an empirical weighting function extracted by as system of aforementioned equations, being RBE values measured by the radiobiologists and $d(y)$ by the physicists in the same radiation fields. $r(y)$ depends on the biological end-point, on the absorbed dose at which the RBE values were measured and on the microdosimetric spectra site diameter. We have used the weighting function shown in figure 5 and published by Loncol et al., which was calculated from radiobiological RBE values of early effects in mice at 8 Gy and microdosimetric spectra in 2 μm site [6]. We have assumed that the spectra differences between 2 μm and 1 μm sites are negligible. $d(y_i)$ is the weighted probability density at y_i and the index i runs along all the measured and extrapolated channels.

$r(y)$ values 1 up to 10 $\text{keV}/\mu\text{m}$, it reaches a maximum of 4.5 at about 70 $\text{keV}/\mu\text{m}$ and becomes less than 1 for y -values larger than 250 $\text{keV}/\mu\text{m}$. This last fact is interpreted as an over-killing effect of very large y -values The accuracy of $r(y)$ depends on the y -value, being rather low for y -values more than about 250 $\text{keV}/\mu\text{m}$.

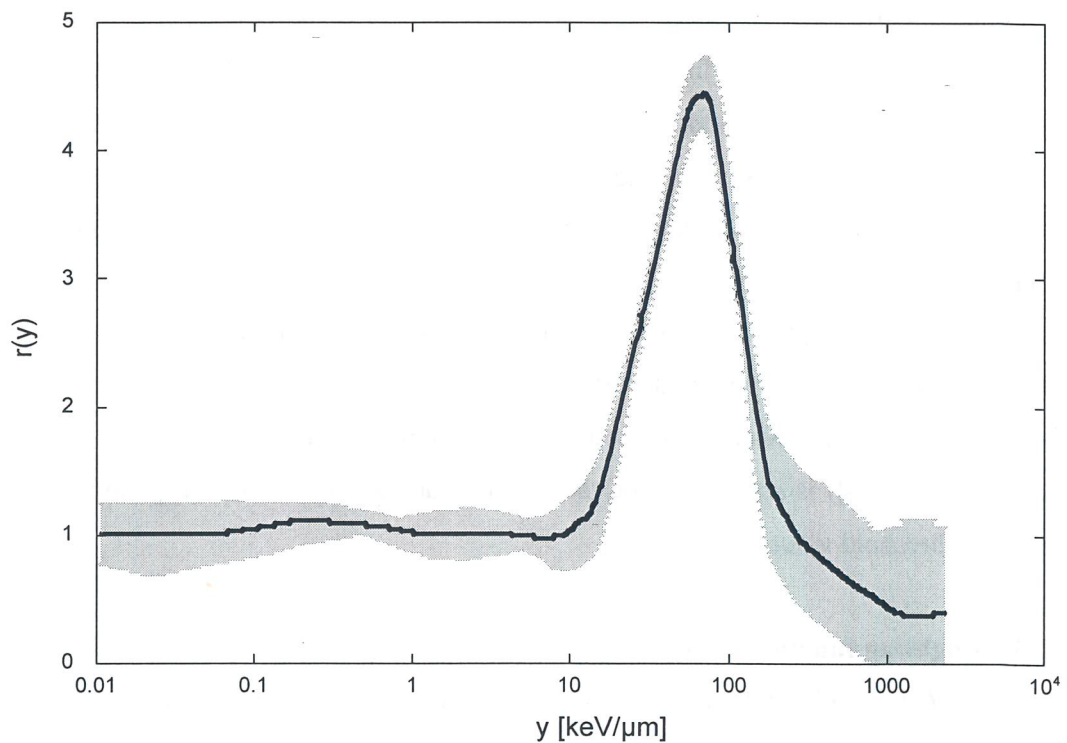


Figure 5. Function to weight the density probability function $d(y)$ in 2 μm of size in order to calculate the early intestine damage in mice at 8 Gy (thick line). The shadow area around the line is ± 1 SD [6].

The uncertainties plotted in figure 6 are not symmetric, being $+SD \neq -SD$. For calculating the overall RBE_μ uncertainty we have taken the maximum SD value at any point (SD_{max}) and substituted the uncertainties of figure 6 with $\pm SD_{\text{max}}$

4. Overall uncertainty of $\overline{y_f}$

The mean lineal energy of the discrete stochastic variable y is:

$$\overline{y_f} = \sum_{0.01}^{y_{\max}} y_i \cdot f(y_i) \cdot \Delta y_i \quad (2)$$

where y_{\max} is the maximum of lineal energy of microdosimetric spectrum (in keV/ μm) and 0.01 (in keV/ μm) is the minimum value at which we extrapolate the frequency spectrum. $f(y_i)$ is the density probability of the y_i -value, which has been counted $n(y_i) \cdot \Delta y_i$ times:

$$f(y_i) = \frac{n(y_i)}{\sum_{0.01}^{y_{\max}} n(y_i) \cdot \Delta y_i} \quad (3)$$

By substituting $f(y_i)$ with the equation (3) and by splitting the equation in a sum of two terms:

$$\overline{y_f} = \frac{\sum_{0.01}^{y_{thr}} y_i \cdot n(y_i)^{extr} \cdot \Delta y_i + \sum_{y_{thr}}^{y_{\max}} y_i \cdot n(y_i) \cdot \Delta y_i}{\sum_{0.01}^{y_{\max}} n(y_i) \cdot \Delta y_i} \quad (4)$$

where y_{thr} is the low experimental threshold value and $n(y_i)^{extr}$ notation remembers that counts from 0.01 keV/ μm up to the threshold y -value are just an extrapolated fit of the last measured counts.

However, as said before, spectra are first processed in Volts and then calibrated in lineal energy by using the calibration factor F_{cal} , which has dimensions keV $\cdot\text{V}^{-1}\cdot\mu\text{m}^{-1}$. By changing the variable $y_i = F_{cal} \cdot \tilde{y}_i$, where \tilde{y} is the y -value in V, and remembering that $n(y_i) \cdot \Delta y_i = n(\tilde{y}_i) \cdot \Delta \tilde{y}_i$, the mean lineal energy can be expressed as:

$$\overline{y_f} = F_{cal} \cdot \frac{\sum_{\tilde{y}_{thr}}^{\tilde{y}_{\max}} \tilde{y}_i \cdot n(\tilde{y}_i)^{extr} \cdot \Delta \tilde{y}_i + \sum_{\tilde{y}_{thr}}^{\tilde{y}_{\max}} \tilde{y}_i \cdot n(\tilde{y}_i) \cdot \Delta \tilde{y}_i}{\sum_{\tilde{y}_{\min}}^{\tilde{y}_{\max}} n(\tilde{y}_i) \cdot \Delta \tilde{y}_i} \quad (5)$$

From the error propagation formula we can obtain the $\overline{y_f}$ relative error:

$$\left(\frac{\sigma_{\overline{y_f}}}{\overline{y_f}} \right)^2 = \left(\frac{\sigma_{F_{cal}}}{F_{cal}} \right)^2 + \left(\frac{\sigma_{\Sigma}}{\Sigma} \right)^2 \quad (6)$$

where the symbol Σ represents the second factor of the right side of the equation (5).

It is no easy to calculate $\left(\frac{\sigma_{\Sigma}}{\Sigma} \right)$, since numerator and denominator of Σ are correlated and therefore:

$$\left(\frac{\sigma_{\Sigma}}{\Sigma}\right)^2 = \left(\frac{\sigma_{num}}{num}\right)^2 + \left(\frac{\sigma_{den}}{den}\right)^2 + 2 \cdot \sigma_{num} \cdot \sigma_{den} \cdot \rho_{corr} \quad (7)$$

where *num* and *den* are respectively the numerator and denominator of Σ whilst ρ_{corr} is the correlation coefficient between numerator and denominator. It is simple to demonstrate that this correlation is negative; that is numerator fluctuations give rise to fluctuation of the same sign at the denominator and consequently the ratio presents a smaller fluctuation. Therefore, if we assume $\rho_{corr}=0$ we overestimate the error.

The error of \tilde{y}_i depends on the *integral linearity* of the electronic chains and the error of $\Delta\tilde{y}_i$ depends on the *differential linearity* of the electronic chains. Before any measurement, both the integral and differential electronic chain linearity are measured with a precise pulser generator and a ramp generator. Microdosimetric measurements are performed only if both the electron chain linearity are good. Therefore, we can disregard the errors on both \tilde{y}_i and $\Delta\tilde{y}_i$.

The error of Σ numerator is the sum of two contributes:

$$\sigma_{num}^2 = \sigma_{extr}^2 + \sigma_{meas}^2 \quad (8)$$

therefore:

$$\left(\frac{\sigma_{y_f}}{y_f}\right)^2 = \left(\frac{\sigma_{F_{cal}}}{F_{cal}}\right)^2 + \left(\frac{\sigma_{extr}}{num}\right)^2 + \left(\frac{\sigma_{meas}}{num}\right)^2 + \left(\frac{\sigma_{den}}{den}\right)^2 \quad (9)$$

where σ_{extr} is the uncertainty of the extrapolation part and σ_{meas} the uncertainty of the measured part of the spectrum. According to the paragraph 3.2 we have:

$$\sigma_{extr}^2 = \left(0.5 \cdot \sum_{\tilde{y}_{min}}^{\tilde{y}_{thr}} \tilde{y}_i \cdot n(\tilde{y}_i)^{extr} \Delta\tilde{y}_i\right)^2 \quad (10)$$

where $n(\tilde{y}_i)^{extr}$ are the count linearly extrapolated by best fitting the last measured points.

σ_{meas} depends only on the fluctuations of $n(\tilde{y}_i)$, since we have assumed that \tilde{y}_i and $\Delta\tilde{y}_i$ have not error. Therefore, remembering that the number of counts per the $\Delta\tilde{y}_i$ interval is $n(\tilde{y}_i) \cdot \Delta\tilde{y}_i$:

$$\sigma_{meas}^2 = \sum_{\tilde{y}_{th}}^{\tilde{y}_{max}} \tilde{y}_i^2 \cdot \Delta\tilde{y}_i \cdot n(\tilde{y}_i) \quad (11)$$

The quadratic error of the denominator is the sum of the quadratic errors of denominator addenda, where the sum runs over all the y-value range. However, we consider only the uncertainties on the experimental data, since the extrapolated counts are usually very large, masking the fluctuations due to the real measured data. Therefore the sum is performed only on the measured y-values.

$$\frac{\sigma_{den}^2}{den^2} = \frac{\sum_{\tilde{y}_{thr}}^{\tilde{y}_{max}} \Delta \tilde{y}_i \cdot n(\tilde{y}_i)}{\left(\sum_{\tilde{y}_{thr}}^{\tilde{y}_{max}} \Delta \tilde{y}_i \cdot n(\tilde{y}_i) \right)^2} \quad (12)$$

Substituting all the components of equation 9, we obtain the relative error of $\overline{y_f}$:

$$\left(\frac{\sigma_{\overline{y_f}}}{\overline{y_f}} \right)^2 = \left(\frac{\sigma_{F_{cal}}}{F_{cal}} \right)^2 + \frac{\left(0.5 \cdot \sum_{\tilde{y}_{min}}^{\tilde{y}_{thr}} \tilde{y}_i \cdot n(\tilde{y}_i)^{extr} \Delta \tilde{y}_i \right)^2}{\left(\sum_{\tilde{y}_{min}}^{\tilde{y}_{max}} \tilde{y}_i \cdot n(\tilde{y}_i) \cdot \Delta \tilde{y} \right)^2} + \frac{\sum_{\tilde{y}_{thr}}^{\tilde{y}_{max}} \tilde{y}_i^2 \cdot \Delta \tilde{y}_i \cdot n(\tilde{y}_i)}{\left(\sum_{\tilde{y}_{min}}^{\tilde{y}_{max}} \tilde{y}_i \cdot n(\tilde{y}_i) \cdot \Delta \tilde{y} \right)^2} + \frac{\sum_{\tilde{y}_{thr}}^{\tilde{y}_{max}} \Delta \tilde{y}_i \cdot n(\tilde{y}_i)}{\left(\sum_{\tilde{y}_{thr}}^{\tilde{y}_{max}} \Delta \tilde{y}_i \cdot n(\tilde{y}_i) \right)^2} \quad (13)$$

By substituting again $\tilde{y} = y / F_{cal}$, the relative overall error of $\overline{y_f}$ can be also written:

$$\left(\frac{\sigma_{\overline{y_f}}}{\overline{y_f}} \right)^2 = \left(\frac{\sigma_{F_{cal}}}{F_{cal}} \right)^2 + \frac{\left(0.5 \cdot \sum_{0.01}^{y_{thr}} y_i \cdot n(y_i)^{extr} \Delta y_i \right)^2}{\left(\sum_{0.01}^{y_{max}} y_i \cdot n(y_i) \cdot \Delta y \right)^2} + \frac{\sum_{y_{thr}}^{y_{max}} y_i^2 \cdot \Delta y_i \cdot n(y_i)}{\left(\sum_{0.01}^{y_{max}} y_i \cdot n(y_i) \cdot \Delta y \right)^2} + \frac{\sum_{y_{thr}}^{y_{max}} \Delta y_i \cdot n(y_i)}{\left(\sum_{y_{thr}}^{y_{max}} \Delta y_i \cdot n(y_i) \right)^2} \quad (14)$$

Where the ratio $\sigma_{F_{cal}}/F_{cal}$ value is 0.036 (see the paragraph 3.1).

The lineal energy calibration factor was $F_{cal}=0.68$ [keV·mV⁻¹·μm⁻¹] in CATANA measurements. The relative uncertainty of the extrapolation (second addendum in equation 9 and 14) has been calculated for the spectrum at 1.6 mm of depth, where it has the maximum of relevance, simulating different threshold values. In table 1 the threshold is given in keV/μm. At deeper depths, the extrapolation procedure uncertainty is less and less important, being about 10⁻⁴ at 25.8 mm of depth for any threshold value.

Table 1. $\overline{y_f}$ relative uncertainty (%) due to low threshold level.

Threshold [keV/μm]	0.14	0.27	0.41	0.54
$\sigma_{extr}/num * 100$	0.4	1.1	2.0	3.7

The last two addenda of equation 14 depend mainly on the count statistics, being the threshold-value dependency rather small. In table 2, the relative contribution of the two addenda (the squared root of their sum: $\sqrt{\left(\frac{\sigma_{max}}{num} \right)^2 + \left(\frac{\sigma_{den}}{den} \right)^2}$) to the overall $\overline{y_f}$ relative uncertainty has been

calculated for the three spectra of figure 1 for a low threshold of 0.2 keV/ μm . In order to assess the count statistics influence on $\frac{\sigma_{\overline{y_f}}}{\overline{y_f}}$, different total count values have been simulated.

For the same statistics, the relative uncertainty decreases at deeper depths. This is probably due to the high y -value rare counts, which are present at smaller depths, because of the higher mean proton energy, which gives rise to some nuclear reactions

Table 2. $\overline{y_f}$ relative uncertainty (%) due to count statistics.

Total counts	10^3	10^4	10^5	10^6	10^7
1.6 mm of depth	16.5	5.2	1.64	0.52	0.16
16.6 mm	10.7	3.4	1.07	0.34	0.11
25.8 mm	9.7	3.1	0.96	0.30	0.10

The overall $\overline{y_f}$ uncertainty depends on the low detection threshold and on the count statistics, as well as on the lineal energy calibration accuracy. The spectrum at 1.6 mm of depth is the most critical, being close to the low detection threshold. Therefore, the relative overall uncertainty of the spectrum at 1.6 mm of depth has been calculated and plotted in figure 6 against the total counts for different low threshold values. Figure 6 shows that the detection threshold of 0.4 keV/ μm and 10^4 counts are enough to obtain a relative uncertainty of about 4%.

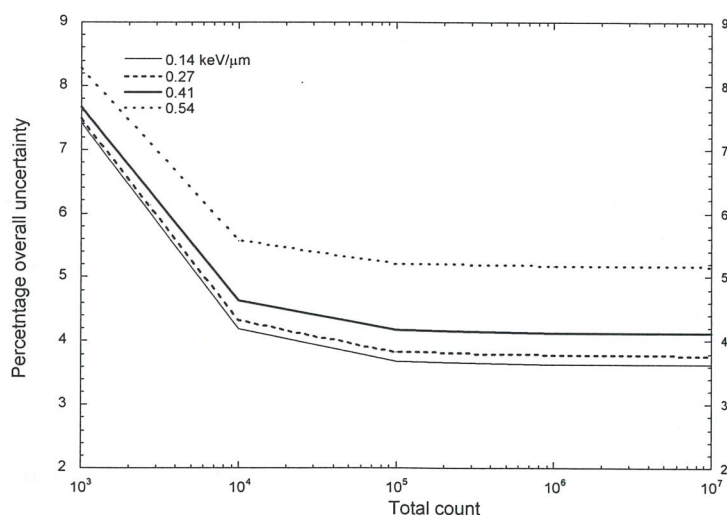


Figure 6. $\overline{y_f}$ overall uncertainty against total counts for microdosimetric spectra collected at 1.6 mm of depth. Different lines correspond to different low detection thresholds, the values of which are reported on the top left side.

5. Overall uncertainty of $\overline{y_d}$

The lineal energy weighted-mean of the discrete stochastic variable y is:

$$\overline{y_d} = \sum_{0.01}^{y_{max}} y_i \cdot d(y_i) \cdot \Delta y_i \quad (15)$$

where y_{max} is the maximum of lineal energy of microdosimetric spectrum (in keV/ μm) and 0.01 (in keV/ μm) is the minimum value at which we extrapolate the frequency spectrum. $d_i(y)$ is the density weighted-probability of the y_i -value, which has been counted $n(y_i) \cdot \Delta y_i$ times:

$$d(y_i) = \frac{y_i \cdot n(y_i)}{\sum_{0.01}^{y_{max}} y_i \cdot n(y_i) \Delta y_i} \quad (16)$$

By substituting $d(y_i)$ with the equation 14 and by splitting the equation in a sum of two terms:

$$\overline{y_d} = \frac{\sum_{0.01}^{y_{thr}} y_i^2 \cdot n(y_i)^{extr} \cdot \Delta y_i + \sum_{y_{thr}}^{y_{max}} y_i^2 \cdot n(y_i) \cdot \Delta y_i}{\sum_{0.01}^{y_{max}} y_i \cdot n(y_i) \cdot \Delta y_i} \quad (17)$$

where y_{thr} is the low experimental threshold. Similarly to that done for $\overline{y_f}$, the calibration factor can be extracted out the sums. Therefore, the lineal energy weighted-mean can be expressed as:

$$\overline{y_d} = F_{cal} \cdot \frac{\sum_{\tilde{y}_{thr}}^{\tilde{y}_{max}} \tilde{y}_i^2 \cdot n(\tilde{y}_i)^{extr} \cdot \Delta \tilde{y}_i + \sum_{\tilde{y}_{thr}}^{\tilde{y}_{max}} \tilde{y}_i^2 \cdot n(\tilde{y}_i) \cdot \Delta \tilde{y}_i}{\sum_{\tilde{y}_{min}}^{\tilde{y}_{max}} \tilde{y}_i \cdot n(\tilde{y}_i) \cdot \Delta \tilde{y}_i} \quad (18)$$

where \tilde{y} is the y -value in V and $F_{cal} [\text{keV} \cdot \mu\text{m}^{-1} \cdot \text{V}^{-1}] = y / \tilde{y}$.

From the error propagation formula:

$$\left(\frac{\sigma_{\overline{y_d}}}{\overline{y_d}} \right)^2 = \left(\frac{\sigma_{F_{cal}}}{F_{cal}} \right)^2 + \left(\frac{\sigma_{\Sigma}}{\Sigma} \right)^2 \quad (19)$$

where Σ is the second term of the equation 17. And then:

$$\left(\frac{\sigma_{\overline{y_d}}}{\overline{y_d}} \right)^2 = \left(\frac{\sigma_{F_{cal}}}{F_{cal}} \right)^2 + \left(\frac{\sigma_{extr}}{num} \right)^2 + \left(\frac{\sigma_{meas}}{num} \right)^2 + \left(\frac{\sigma_{den}}{den} \right)^2 \quad (20)$$

Following for $\overline{y_d}$ the same line of reasoning followed for calculating $\overline{y_f}$ relative overall uncertainty, we eventually obtain:

$$\left(\frac{\sigma_{\overline{y_d}}}{\overline{y_d}} \right)^2 = \left(\frac{\sigma_{F_{cal}}}{F_{cal}} \right)^2 + \frac{\left(0.5 \cdot \sum_{\tilde{y}_{min}}^{\tilde{y}_{thr}} \tilde{y}_i^2 \cdot n(\tilde{y}_i)^{extr} \Delta \tilde{y}_i \right)^2}{\left(\sum_{\tilde{y}_{min}}^{\tilde{y}_{max}} \tilde{y}_i^2 \cdot n(\tilde{y}_i) \cdot \Delta \tilde{y}_i \right)^2} + \frac{\sum_{\tilde{y}_{thr}}^{\tilde{y}_{max}} \tilde{y}_i^4 \cdot \Delta \tilde{y}_i \cdot n(\tilde{y}_i)}{\left(\sum_{\tilde{y}_{min}}^{\tilde{y}_{max}} \tilde{y}_i^2 \cdot n(\tilde{y}_i) \cdot \Delta \tilde{y}_i \right)^2} + \frac{\sum_{\tilde{y}_{thr}}^{\tilde{y}_{max}} \tilde{y}_i^2 \cdot \Delta \tilde{y}_i \cdot n(\tilde{y}_i)}{\left(\sum_{\tilde{y}_{thr}}^{\tilde{y}_{max}} \tilde{y}_i \cdot \Delta \tilde{y}_i \cdot n(\tilde{y}_i) \right)^2} \quad (21)$$

By substituting again $\tilde{y} = y / F_{cal}$, the relative overall error of $\overline{y_d}$ can be also written:

$$\left(\frac{\sigma_{\overline{y_d}}}{\overline{y_d}}\right)^2 = \left(\frac{\sigma_{F_{cal}}}{F_{cal}}\right)^2 + \frac{\left(0.5 \cdot \sum_{0.01}^{y_{thr}} y_i^2 \cdot n(y_i)^{extr} \Delta y_i\right)^2}{\left(\sum_{0.01}^{y_{max}} y_i^2 \cdot n(y_i) \cdot \Delta y\right)^2} + \frac{\sum_{y_{thr}}^{y_{max}} y_i^4 \cdot \Delta y_i \cdot n(y_i)}{\left(\sum_{0.01}^{y_{max}} y_i^2 \cdot n(y_i) \cdot \Delta y\right)^2} + \frac{\sum_{y_{thr}}^{y_{max}} y_i^2 \cdot \Delta y_i \cdot n(y_i)}{\left(\sum_{y_{thr}}^{y_{max}} y_i \cdot \Delta y_i \cdot n(y_i)\right)^2} \quad (22)$$

Where the ratio $\sigma_{F_{cal}}/F_{cal}$ is ad usual 0.036 (see paragraph 3.1).

The extrapolation procedure error plays a minor role for $\overline{y_d}$. In table 3 the extrapolation relative uncertainty, calculated for the spectrum at 1.6 mm of depth, have been calculated for different simulated low threshold values. Results show that unlikely this error can be more than 1%.

Table 3. $\overline{y_d}$ relative uncertainty (%) due to low threshold level.

Threshold [keV/ μ m]	0.14	0.27	0.41	0.54
$\sigma_{extr}/num * 100$	0.007	0.036	0.11	0.3

The last two addenda of equation 20 depend mainly on the count statistics, being the threshold-value dependency rather small. In table 4, the relative contribution of the two addenda (the squared root of their sum: $\sqrt{\left(\frac{\sigma_{num}}{num}\right)^2 + \left(\frac{\sigma_{den}}{den}\right)^2}$) to the overall $\overline{y_d}$ relative uncertainty has been calculated for the three spectra of figure 1 and for different total counts (for a low threshold of 0.2 keV/ μ m).

Table 4. $\overline{y_d}$ relative uncertainty (%) due to count statistics.

Total counts	10^3	10^4	10^5	10^6	10^7
1.6 mm of depth	272	86	27.2	8.6	2.72
16.6 mm	81.7	25.8	8.17	2.58	0.82
25.8 mm	11.0	3.48	1.10	0.35	0.11

For the same statistics, the count-due relative uncertainty decreases with the depth. This decrease is sharper than that one for $\overline{y_f}$. The rare high y-value counts, which are present at smaller depths, play in fact a bigger role in calculating $\overline{y_d}$. Because of that, a larger statistics is necessary to obtain accurate $\overline{y_d}$ -values at 1.6 mm of depth.

In figure 7, the $\overline{y_d}$ overall relative uncertainty is plotted against the total counts and for different depths. An accurate ($\sim 4\%$) $\overline{y_d}$ value is obtainable with 10^6 counts in the SOBP, and even with less counts in the SOBP distal edge. However, to obtain a similarly accurate $\overline{y_d}$ value at the beam entrance, more than 10^7 counts are necessary.

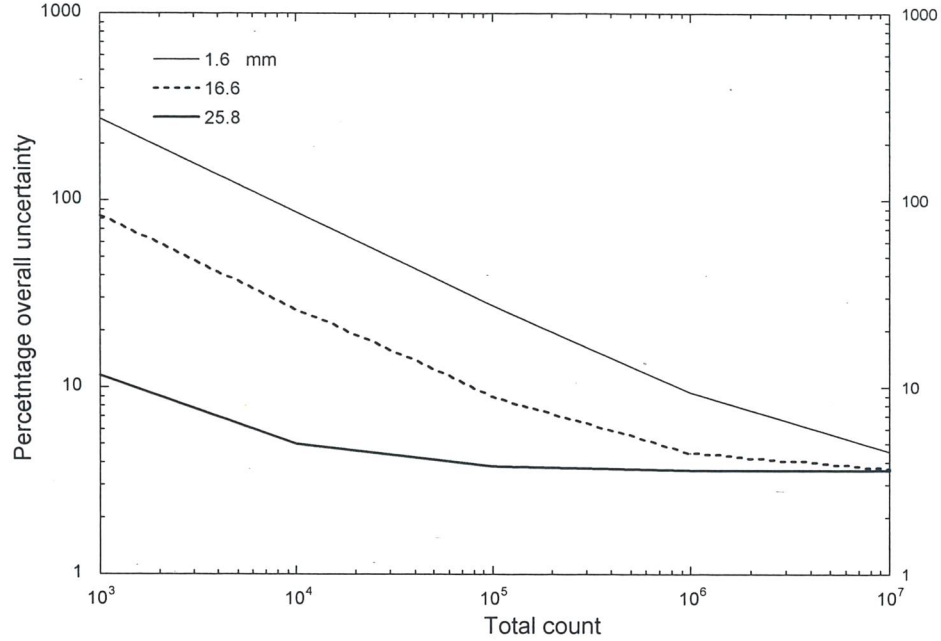


Figure 7. $\overline{y_d}$ overall uncertainty against total counts. Different line corresponds to a different microdosimetric spectrum collected at the depth shown on the top left side.

6. Overall uncertainty of RBE_μ

Remembering the RBE_μ definition (equation 1) and the $d(y)$ definition (equation 14), we obtain the explicit RBE_μ definition:

$$RBE_\mu = \frac{\sum_{y_{thr}}^{y_{th}} r(y_i) \cdot y_i \cdot n(y_i)^{extr} \cdot \Delta y_i + \sum_{y_{thr}}^{y_{max}} r(y_i) \cdot y_i \cdot n(y_i) \cdot \Delta y_i}{\sum_{0.01}^{y_{max}} y_i \cdot n(y_i) \cdot \Delta y_i} \quad (23)$$

In equation 23 we can not changing everywhere the y -variable by using the equation $y_i = F_{cal} \cdot \tilde{y}_i$, since $r(y_i)$ is a literature function [6] given in keV/ μm not in Volt. However, the weighting function $r(y_i)$ is 1 for $y < 10$ keV/ μm (see figure 5). Since we can assume that the low threshold y_{thr} is always less than 10 keV/ μm , we can simplify the equation 23 and obtaining:

$$RBE_{\mu} = \frac{\sum_{y_i}^{y_{thr}} y_i \cdot n(y_i)^{extr} \cdot \Delta y_i + \sum_{y_i}^{y_{max}} r(y_i) \cdot y_i \cdot n(y_i) \cdot \Delta y_i}{\frac{0.01}{y_{thr}} \sum_{y_i}^{y_{max}} y_i \cdot n(y_i) \cdot \Delta y_i} \quad (24)$$

Now we can substitute y with \tilde{y} , where it is possible:

$$RBE_{\mu} = \frac{F_{cal} \cdot \sum_{\tilde{y}_i}^{\tilde{y}_{thr}} \tilde{y}_i \cdot n(\tilde{y}_i)^{extr} \cdot \Delta \tilde{y}_i + \sum_{y_i}^{y_{max}} r(y_i) \cdot y_i \cdot n(y_i) \cdot \Delta y_i}{F_{cal} \cdot \sum_{\tilde{y}_i}^{\tilde{y}_{max}} \tilde{y}_i \cdot n(\tilde{y}_i) \cdot \Delta \tilde{y}_i} \quad (25)$$

From the error propagation formula, we obtain:

$$\left(\frac{\sigma_{RBE_{\mu}}}{RBE_{\mu}} \right)^2 = \left(\frac{\sigma_{num}}{num} \right)^2 + \left(\frac{\sigma_{den}}{den} \right)^2 \quad (26)$$

where *num* and *den* have the usual meaning. The numerator is made of two addenda, therefore:

$$\sigma_{num}^2 = \sigma_{extr}^2 + \sigma_{meas}^2 \quad (27)$$

Since the numerator first addendum (*extr*) is in its turn the product of two factors:

$$\sigma_{extr}^2 = \left(\frac{\sigma_{F_{cal}}^2}{F_{cal}^2} + \frac{\sigma_{extr(\tilde{y})}^2}{extr(\tilde{y})^2} \right) \cdot extr^2 \quad (28)$$

where *extr*(\tilde{y}) is the sum and *extr* is the sum multiplied by the calibration factor F_{cal} . Substituting and applying the usual reasoning to get $\sigma_{extr(\tilde{y})}$, we obtain:

$$\sigma_{extr}^2 = \left(\frac{\sigma_{F_{cal}}^2}{F_{cal}^2} + \frac{\left(0.5 \cdot \sum_{\tilde{y}_i}^{\tilde{y}_{thr}} \tilde{y}_i \cdot n(\tilde{y}_i)^{extr} \cdot \Delta \tilde{y}_i \right)^2}{\left(\sum_{\tilde{y}_i}^{\tilde{y}_{thr}} \tilde{y}_i \cdot n(\tilde{y}_i)^{extr} \cdot \Delta \tilde{y}_i \right)^2} \right) \cdot \left(F_{cal} \cdot \sum_{\tilde{y}_i}^{\tilde{y}_{thr}} \tilde{y}_i \cdot n(\tilde{y}_i)^{extr} \cdot \Delta \tilde{y}_i \right)^2 \quad (29)$$

and eventually, remembering that \tilde{y}_{min} corresponds to 0.01 keV/ μ m:

$$\sigma_{extr}^2 = \left(\frac{\sigma_{F_{cal}}^2}{F_{cal}^2} + 0.25 \right) \cdot \left(\sum_{y_i}^{y_{thr}} y_i \cdot n(y_i)^{extr} \cdot \Delta y_i \right)^2 \quad (30)$$

In the numerator of equation 25, the y -variable in the second addendum (*meas*) is in keV/ μ m, therefore to assess σ_{meas}^2 we first sum the relative squared error of $r(y_i)$ and $n(y_i)$ and then we add the absolute squared error due to calibration uncertainty. Remembering that $n(y)$ is a count density:

$$\sigma_{meas}^2 = \left(\frac{\sigma_{r(y)}^2}{r^2(y)} + \frac{\sigma_{\Delta y \cdot n(y)}^2}{\Delta y^2 \cdot n^2(y)} \right) \cdot meas^2 + \sigma_{cal}^2 \quad (31)$$

The calibration uncertainty σ_{cal}^2 is assessed as the impact of the lineal-energy calibration uncertainty on the product $r(y) \cdot y \cdot n(y)$. To do that, the multiplication is performed once with $n^+(y_i)$ and another time with $n^-(y_i)$. Where $n^+(y_i)$ is the count density corresponding to the $y_i + \sigma_F$ value and $n^-(y_i)$ is the count density corresponding to the $y_i - \sigma_F$ value, being σ_F the lineal energy standard deviation (see paragraph 4). The uncertainty is then assumed to be half of the difference of the two products. This uncertainty is therefore half of the maximum error, but only if the function $n(y)$ is monotone, which is not true in general, but $n(y)$ varies so smoothly that it can be assumed monotone inside the range $y_i - \sigma_F < y_i < y_i + \sigma_F$. Therefore:

$$\sigma_{meas}^2 = \sum_{y_{thr}}^{y_{max}} \left(\frac{\sigma_{r_i}^2}{r_i^2} + \frac{1}{\Delta y_i \cdot n(y_i)} \right) \cdot r^2(y_i) \cdot y_i^2 \cdot n^2(y_i) \cdot \Delta y_i^2 + 0.25 \cdot r^2(y_i) \cdot y_i^2 \cdot \Delta y_i^2 \cdot [n^+(y_i) - n^-(y_i)]^2 \quad (32)$$

and simplifying

$$\sigma_{meas}^2 = \sum_{y_{thr}}^{y_{max}} \left[\frac{\sigma_{r_i}^2}{r_i^2} \cdot n^2(y_i) + \frac{n(y_i)}{\Delta y_i} + 0.25 \cdot [n^+(y_i) - n^-(y_i)]^2 \right] \cdot r^2(y_i) \cdot y_i^2 \cdot \Delta y_i^2 \quad (33)$$

The denominator of equation 25 is a normalisation factor, the uncertainty of which depends both on the $n(\tilde{y})$ statistics and on the calibration factor uncertainty. The calibration factor can be taken out of the sum, therefore, taking into account the observation used for the equation 12:

$$\left(\frac{\sigma_{den}}{den} \right)^2 = \frac{\sigma_{F_{cal}}^2}{F_{cal}^2} + \frac{\sum_{\tilde{y}_{thr}}^{\tilde{y}_{max}} \tilde{y}_i^2 \cdot \Delta \tilde{y}_i \cdot n(\tilde{y}_i)}{\left(\sum_{\tilde{y}_{thr}}^{\tilde{y}_{max}} \tilde{y}_i \cdot \Delta \tilde{y}_i \cdot n(\tilde{y}_i) \right)^2} \quad (34)$$

Where we have substituted \tilde{y}_{min} with \tilde{y}_{thr} for preventing the “masking effect” due to extrapolated counts. Since $y = F_{cal} \cdot \tilde{y}$, the relative denominator uncertainty is also:

$$\left(\frac{\sigma_{den}}{den} \right)^2 = \frac{\sigma_{F_{cal}}^2}{F_{cal}^2} + \frac{y_{thr} \sum_{y_i}^{y_{max}} y_i^2 \cdot \Delta y_i \cdot n(y_i)}{\left(\sum_{y_{thr}}^{y_{max}} y_i \cdot \Delta y_i \cdot n(y_i) \right)^2} \quad (35)$$

Differently from $\overline{y_f}$ and $\overline{y_d}$ uncertainties, the RBE_μ overall uncertainty can not be separated in its three components; namely the threshold, lineal energy and count uncertainties. Therefore, it is convenient to calculate the overall RBE_μ relative uncertainty by using $n(y)$ rather than $n(\overline{y})$. If we call A the second term of the equation 30 and B the second term of the equation 33, we obtain:

$$\frac{\sigma_{RBE}^2}{RBE_\mu^2} = \frac{A + B}{\left(\sum_{0.01}^{y_{\max}} r(y_i) \cdot y_i \cdot n(y_i) \cdot \Delta y_i \right)^2} + \frac{\sigma_{F_{cal}}^2}{F_{cal}^2} + \frac{\sum_{y_{th}}^{y_{\max}} y_i^2 \cdot \Delta y_i \cdot n(y_i)}{\left(\sum_{y_{th}}^{y_{\max}} y_i \cdot \Delta y_i \cdot n(y_i) \right)^2} \quad (36)$$

where the lineal energy calibration uncertainty is also present both in A and on B .

RBE_μ uncertainty depends on the low threshold level as more as more counts have low y -value, as in the microdosimetric spectrum at 1.6 mm of depth. In table 5 the overall relative RBE_μ uncertainty has been calculated for the spectrum at 1.6 mm of depth for statistics of 10^6 counts.

Table 5. RBE_μ overall relative uncertainty (%) for different low threshold levels.

Threshold [keV/ μ m]	0.14	0.27	0.41	0.54
$\sigma_{RBE_\mu} / RBE_\mu * 100$	4.12	4.18	4.48	5.21

At deeper depths, the extrapolation error does not change significantly $\sigma_{RBE_\mu} / RBE_\mu$, as expected.

In table 6, the overall RBE_μ relative uncertainty has been calculated for the three spectra of figure 1 for different statistics and for a low threshold of 0.2 keV/ μ m.

Table 6. RBE_μ overall relative uncertainty (%) for different count statistics.

Total counts	10^3	10^4	10^5	10^6	10^7
1.6 mm of depth	11.4	5.33	4.26	4.14	4.12
16.6 mm	12.3	5.51	4.27	4.13	4.12
25.8 mm	9.07	4.83	4.18	4.11	4.10

The data are plotted in figure 8. It is possible to observe that relative RBE_μ overall uncertainty converges to the value of $\sim 4\%$ already at 10^5 counts, for any depth, when the low threshold is of 0.2 keV/ μ m. If higher low threshold values, the RBE_μ uncertainty converges

towards higher values: $\sim 5\%$ for the $0.5 \text{ keV}/\mu\text{m}$ threshold and 1.6 mm of depth, $\sim 9\%$ for $0.8 \text{ keV}/\mu\text{m}$ and so on.

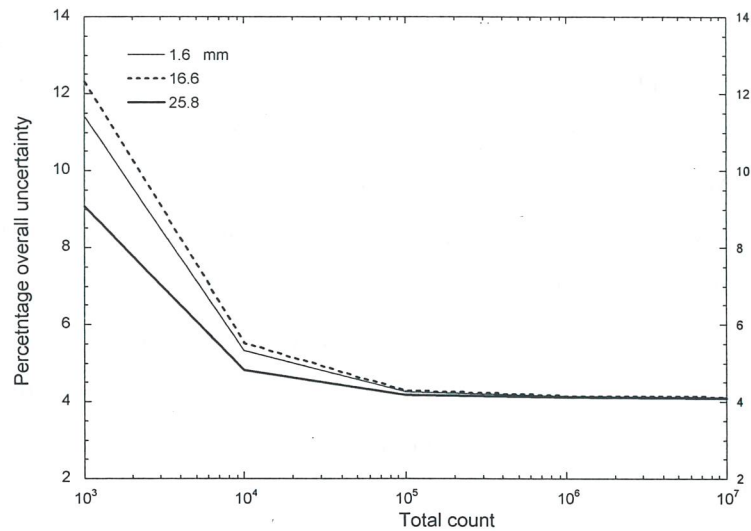


Figure 8. RBE_μ relative overall uncertainty against different total counts. Different lines correspond to different depths.

7. Conclusions

We have calculated the overall uncertainties of $\overline{y_f}$, $\overline{y_d}$ and RBE_μ of therapeutic proton spectra. We have taken into account the lineal energy calibration uncertainty, the uncertainty related to the spectrum extrapolation down to $0.01 \text{ keV}/\mu\text{m}$ and the statistical uncertainty.

If the low detection threshold is $0.2 \text{ keV}/\mu\text{m}$ or less, 10^5 counts are enough to obtain the relative overall uncertainty of $\sim 4\%$ both for $\overline{y_f}$ and RBE_μ at any depth. More critical is the $\overline{y_d}$ calculation, since more than 10^7 counts are necessary to obtain 4% of relative overall uncertainty at any depth.

References

- [1] International Commission on Radiation Units and Measurements(ICRU) Report 36, *Microdosimetry*, 1983
- [2] International Commission on Radiation Units and Measurements. Stopping powers and ranges for protons and alpha particles. Report 49. Bethesda, MD. ICRU Publications (1993).
- [3] Comité International des Poids et Mesures, Procès-Verbaux 49, A11, 1981.
- [4] Giacomo, P. *News from the BIPM*. Metrologia 17, 69 (1981).
- [5] De Nardo, L., Cesari, V., Donà, G., Colautti, P., Conte, V. and Tornielli, G. *Mini TEPCs for proton therapy*. Submitted to Radiat. Prot. Dosim. (2003).
- [6] Loncoln, T., Cosgrove, V., Denis, J.M., Gueulette, J., Mazal, A., Menzel, H.G., Pihet, P. and Sabattier, R. *Radiobiological Effectiveness of Radiation Beams with Broad LET Spectra: Microdosimetric Analysis Using Biological Weighting Functions*. Radiat. Prot. Dosim. 52, 347-352 (1994).